



HAL
open science

Thermal Transistor Effect in Quantum Systems

Antonio Mandarino, Karl Joulain, Melisa Domínguez Gómez, Bruno Bellomo

► **To cite this version:**

Antonio Mandarino, Karl Joulain, Melisa Domínguez Gómez, Bruno Bellomo. Thermal Transistor Effect in Quantum Systems. *Physical Review Applied*, 2021, 16 (3), pp.034026. 10.1103/PhysRevApplied.16.034026 . hal-03543570

HAL Id: hal-03543570

<https://hal.science/hal-03543570>

Submitted on 26 Apr 2023

HAL is a multi-disciplinary open access archive for the deposit and dissemination of scientific research documents, whether they are published or not. The documents may come from teaching and research institutions in France or abroad, or from public or private research centers.

L'archive ouverte pluridisciplinaire **HAL**, est destinée au dépôt et à la diffusion de documents scientifiques de niveau recherche, publiés ou non, émanant des établissements d'enseignement et de recherche français ou étrangers, des laboratoires publics ou privés.

Thermal transistor effect in quantum systems

Antonio Mandarino,¹ Karl Joulain,² Melisa Domínguez Gómez,^{2,3} and Bruno Bellomo¹

¹*Institut UTINAM - UMR 6213, CNRS, Université Bourgogne Franche-Comté,*

Observatoire des Sciences de l'Univers THETA, 41 bis avenue de l'Observatoire, F-25010 Besançon, France

²*Insitut Pprime, CNRS, Université de Poitiers, ISAE-ENSMA, F-86962 Futuroscope Chasseneuil, France*

³*Instituto de Física, Universidad de Antioquia, Calle 70 No. 52-21, Medellín, Colombia*

We study a quantum system composed of three interacting qubits, each coupled to a different thermal reservoir. We show how to engineer it in order to build a quantum device that is analogous to an electronic bipolar transistor. We outline how the interaction among the qubits plays a crucial role for the appearance of the effect, also linking it to the characteristics of system-bath interactions that govern the decoherence and dissipation mechanism of the system. By comparing with previous proposals, the model considered here extends the regime of parameters where the transistor effect shows up and its robustness with respect to small variations of the coupling parameters. Moreover, our model appears to be more realistic and directly connected in terms of potential implementations to feasible setups in the domain of quantum spin chains and molecular nanomagnets.

I. INTRODUCTION

The exploitation of classical thermodynamics has conducted to the technological revolution that shaped our world since the Nineteenth century [1]. In recent years the exploration of the thermodynamics of quantum systems has given birth to quantum thermodynamics: a high impact research field either on the fundamental level and the applicative one [2]. In analogy to classical models, quantum heat engines have been proposed and realized [3–5]. In particular, the properties of non-equilibrium open quantum systems has been employed to study how to obtain many-body entanglement [6] or efficient flux management [7]. Moreover, the implementation of non-equilibrium quantum heat machines has been discussed in solid state set-ups [8] or in more complex scenarios [9].

The ability to manipulate quantum resources is a demanding but fruitful task that has to be pursued in order to build novel devices. A potential high impact apparatus will be the one aiming at the control of thermal energy transport in quantum systems, and at the amplification of heat fluxes among the different parts constituting a composite system. A promising approach in the aforementioned task is to pursue the flourishing path followed in electronics after the realization of rectifiers and transistors with semi-conducting materials [10] that paved the way to build logic gates and to the information and computational technology [11].

Typically, thermal and electric currents phenomena are empirically well described by the Fourier's and Ohm's laws, respectively. In fact, the functional dependence upon the two respective control variables, temperature and voltage, is of the same type. Recently, evidences of the emergence of the Fourier's law has been pointed out also in the quantum realm [12, 13].

The proposal of such thermal analogues of the electronic rectifier and transistor is based on the assumption that in a thermal set-up the role played by batteries could be played by thermostats. This analogy allowed to come forward with various proposals of mesoscopic thermal de-

vices such as rectifiers and diodes [14, 15] and transistors [16], the latter operating either in near field [17] or in far field [18] regime of thermal radiation, and also thermal logic gates [19, 20].

The theoretical efforts are bolstered by the experimental ingenuity involving a wide range of experimental platforms ranging from carbon and boron nitride nanotube structures [21] and bulk oxide materials [22] to semiconductors quantum dots [23], magnonic systems [24] and phase changing materials, such as vanadium dioxide VO₂ [25, 26], and ceramics materials that below a critical temperature behave like high temperature superconductors and above it as dielectrics [27, 28].

In the same time, the quest of atomic-scale devices for quantum computational purposes is increasingly pushing the necessity to control and manipulate single or few atoms systems. In particular, the isolation and coherent manipulation of single spins, that are one of the best candidates for a non-optical implementation of a single qubit, is achieved using optical traps and electrical techniques [29]. Recently, several novel quantum technology devices have been proposed, including isolators based on photonic transitions [30], rectifiers [31, 32], transistors in an electromagnetic controlled environment [33, 34], and also phonon-thermoelectric transistors [35].

Moreover, quantum systems suffer of an unavoidable coupling to their environment, typically modeled as a thermal reservoir of much bigger dimensions of those of the system [36, 37]. Despite some detrimental phenomena related to decoherence and dissipation, control and engineering of interacting quantum systems coupled with different thermal baths have led to several studies pointing out how to build the smallest thermal refrigerator [38, 39], how to rectify a thermal current at the very quantum level [40–42] and recently the building blocks of a quantum thermal transistor have been discussed considering an integrable spin-chain model [43] and in a qubit-qutrit system [44].

In this paper we analyze the ability to design a quantum thermal transistor employing a spin ring that can, in principle, be implemented on a molecular nanomagnet

[45]. In comparison to a previous model [43], we consider a more complex scenario where the collective quantum behavior of few spins is expected to play a crucial role in the functioning of the device.

The paper is structured as follows. In Section II, we examine the spin-ring model outlining the frameworks where the theoretical model finds a direct implementability. This section is also devoted to the quantum dissipative process that allows the system to exchange heat fluxes. In Section III, we discuss how the proposed systems can be adopted to build a quantum thermal transistor and some limits of their applicability. Having in mind a direct experimental implementation, in Section IV the robustness of the transistor effect against unavoidable fluctuations and perturbations is addressed. Section V concludes the paper with some final remarks and prospects. Some details can be found in the Appendix.

II. THE SPIN-RING MODEL

Quantum critical spin chains have longly been considered as one of the best substrates to test and implement the future quantum computing and the novel quantum devices. Their main characteristic is to show wide versatility [46]. In fact, considering the most general model for quantum magnetism, described by the Heisenberg Hamiltonian, one can explore a great variety of universality class by an appropriate tuning of the interaction strengths. Moreover, recent modern developments allow to realize spin chains of few atoms having net spin $s = 1/2$, opening the road to the exploitation of the physics of some well known models, viz., Ising, XY and XXZ ones [47–51].

In parallel, molecular nanomagnets [45] are also attracting more interest as a feasible platform for quantum technological purposes [52]. Specifically, molecular nanomagnets, composed by $N = 3$ main units, have been proved to be useful for quantum thermometry [53] and for coherent-manipulation of three-qubit states [54].

Spin chains and nanomagnets are theoretically well described by the same effective Hamiltonian upon fixing the configuration geometry. Here, we consider a system of three two-level systems (qubits) of frequency ω_p ($p = L, M, R$), embedded in a magnetic field, and we introduce the vector of the effective spin operators of any qubit $\hat{\mathbf{S}}_p = (\sigma_p^x, \sigma_p^y, \sigma_p^z)^T$ and the 3-by-3 matrix $\boldsymbol{\lambda}$ governing the coupling between spins along different polarization axis, where σ_p^i ($i = x, y, z$) is the i -th Pauli matrix of the p -th qubit. A realistic description of a triangular spin chain with a qubit in each vertex labeled L, M and R , as depicted in Fig. 1, is given by the following Hamiltonian (hereafter the reduced Plank constant and the Boltzmann constant are set equal to one, $\hbar = k_B = 1$):

$$H_S = \frac{1}{2} \sum_{p=L,M,R} \omega_p \sigma_p^z + \sum_{p \neq q} \hat{\mathbf{S}}_p^T \boldsymbol{\lambda} \hat{\mathbf{S}}_q. \quad (1)$$

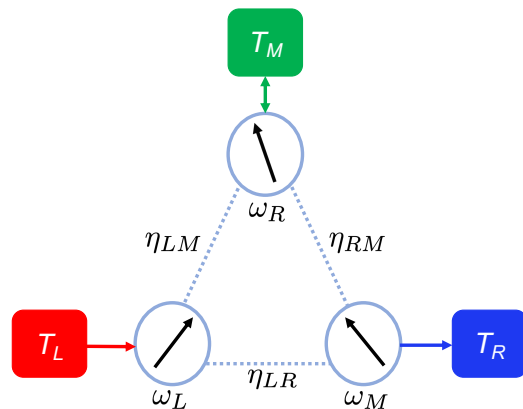


FIG. 1: (Color online) Schematic picture of a system composed by three qubits interacting each one with any other according to the model in Eq. (2). Each of them is dissipating into a different thermal environment as described in Eq. (3).

The first term is the sum of single particle *free* Hamiltonians of three qubits immersed in a magnetic field pointing along the direction of the z -axis and it is responsible of the non-zero field splitting of each qubit, while the second term is the intra-chain spin-spin exchange coupling. Such an Hamiltonian takes into account symmetric and antisymmetric exchange interactions. A proper tuning of $\boldsymbol{\lambda}$ can give a situation where only the former type of interactions occurs, like in the standard Heisenberg Hamiltonian, or can introduce a coupling between non-homologous components of the spin operators, as in the Dzyaloshinskii-Moriya interaction [55, 56]. We omit here the overcomplexity introduced by an antisymmetric exchange, hence we assume that the tensor $\boldsymbol{\lambda}$ contains only symmetric terms.

This allows us to consider spins interacting among them through an Heisenberg type Hamiltonian. Therefore, specifying their couplings η_{pq} with $p, q = L, M, R$ and $p \neq q$, and the strengths along different polarization axis λ^i , the Hamiltonian of the system reads:

$$H_S = \frac{1}{2} \sum_{p=L,M,R} \omega_p \sigma_p^z + \frac{1}{2} \sum_{p \neq q} \eta_{pq} \sum_{i=x,y,z} \lambda^i \sigma_p^i \sigma_q^i, \quad (2)$$

where we have chosen equal λ^i for the three qubits.

This Hamiltonian describes the simplest non-trivial example of spin ring whose properties can be observed with good approximation in a $\{\text{Cu}_3\}$ -Type nanomagnet, a complex having an almost equilateral triangular shape with a Cu^{2+} ion of spin-1/2 at each vertex [57].

A. Comparison between two Ising-type rings

Joulain et al. in their seminal paper [43] have addressed how a thermal transistor can be realized with a quantum system of three interacting qubits, coupled to a thermal reservoir each, and showed how it is analogous

to an electronic bipolar one. Their discussion is based on a peculiar choice of a very simple model, that implies a lot of strong assumptions on the underlying physics.

Let us refer to the model adopted in [43] as the z -axis. In fact, there the magnetic field applied on the three qubits is longitudinal to the direction of the spin-spin interactions. Being more specific, the exchange interaction in H_S of Eq. (2) is non-zero only along the same direction of the magnetic field, i.e. only $\lambda^z \neq 0$. Among the other assumptions, this is the one that, in our opinion, requires now a detailed discussion. In fact, this premise, along with some other minor approximations, has the advantage to let the model and the dissipative dynamics be solvable with analytical techniques, since the operators $\sigma_p^z \sigma_q^z$ commute with the free Hamiltonian. Essentially, the only effect of the zero field splitting terms $\sigma_p^z \sigma_q^z$ is to modify the eigenenergies of the system, but the collective eigenfunctions remain the same and can be still expressed as a tensor product of single-particle eigenstates. We note that this kind of spin ring, even if considered in a quantum context, is a semi-classical model. In fact, the spin-1/2 operators σ_p^z can be alternatively viewed as a classical magnetic moment pointing only along two opposite directions. The z -axis Ising model, hence, takes correctly into account a quantization of the magnetic moment, but it does not consider quantum fluctuations due to other spatial components of the same spin operator \hat{S}_p and any possible critical behavior is disregarded.

It is worth noting that in order to propose a truly quantum model a more complex interaction should be taken into account. The reason why we discuss the class of Hamiltonians defined in Eq. (2), where, in general, the sum of the single particle contributions does not commute with the interaction term is twofold: (i) from a purely theoretical point of view, these systems may exhibit strongly correlated and nonlocal eigenstates, opening the door to phenomena with an enhancement due to quantum correlations or criticality [46]; (ii) from an experimentally inspired perspective, nowadays, the control of nanomagnets, spin chains or even quantum dot molecules, has been well established for quantum critical systems [49–51].

For the aforementioned reasons our aim is then to propose a well established quantum setting, richer than the one considered in [43], where the thermal transistor effect displays and to study its robustness with respect to the operating temperature and against spurious fluctuations of the exchange interactions.

In particular, we will mainly focus on the case of magnetic systems that belong to the universality class of the quantum critical Ising model in a transverse field and we will refer shorthand to it as the x -axis Ising model. It can be realized considering in Eq. (2) that the coupling among the qubits acts only along a direction (that we name x) transverse to the applied magnetic field, i.e. only $\lambda^x \neq 0$. We remark that once the coupling with the environment is added (see next sub-section), the different directions transverse to the applied magnetic field

are not equivalent anymore. We address in Section IV the presence of perturbations on both the x and z configurations.

The x -axis Ising model introduced as the exemplary model to study quantum phase transitions in magnetic systems and their critical behaviors has been employed in a wide range of protocols to characterize and fulfill quantum computational tasks [46]. The main feature of such a model resides in the fact that its collective states are no longer a tensor product of the single particles states, but are non-separable. Its pivotal role for the comprehension of magnetism at the quantum scale has fostered the research of a model magnet where its properties can be experimentally measured with different techniques. Nowadays, the most germane realization has been achieved in the low-energy magnetic excitation of the insulator LiHoF₄ [49] or with crystals of the ferromagnetic CoNb₂O₆ where the spin resides on the Co²⁺ ion [50]. A detailed presentation of the spectrum of the x -axis Ising model for the purposes of this paper is shown in Appendix , while a complete discussion of the spectrum of z -axis one can be found in [43].

B. Dissipative dynamics

Each qubit composing the spin ring described above suffers of an unavoidable coupling with its surrounding environment, that is modeled as a thermal bosonic reservoir. The temperatures of the three reservoirs are, in general, different, giving rise to an out of thermal equilibrium scenario where the temperatures are meant to be tunable at will. The total Hamiltonian is then $H = H_S + H_B + H_I$, where the bath and the system-bath Hamiltonians, respectively, read:

$$\begin{aligned} H_B &= \sum_{p=L,M,R} \sum_k \omega_k a_k^{p\dagger} a_k^p \\ H_I &= \sum_{p=L,M,R} \sigma_p^x \otimes \sum_k g_k^p (a_k^{p\dagger} + a_k^p), \end{aligned} \quad (3)$$

where a_k^p and $a_k^{p\dagger}$ are the bosonic operators of bath p and g_k^p are the coupling strengths. A schematic representation of the global system is sketched in Fig. 1. As spin ring Hamiltonian H_S , we consider the one of Eq. (2).

The dynamics of the 3-qubit system is dissipative and, under the Born-Markov and secular approximations [36], the evolution of the density matrix is described by a master equation of the following form:

$$\dot{\rho} = -i[H_S + H_{LS}, \rho] + \sum_{p=1}^3 \mathcal{L}_p[\rho], \quad (4)$$

where $H_{LS} = \sum_{p,\omega} s_p(\omega) A_p^\dagger(\omega) A_p(\omega)$ is the Lamb shift Hamiltonian, $A_p(\omega) = \sum_{\omega=\epsilon_i-\epsilon_j} |\epsilon_j\rangle \langle \epsilon_j| \sigma_p^x |\epsilon_i\rangle \langle \epsilon_i|$, $|\epsilon_i\rangle$ with $i = 1, \dots, 8$ are the dressed states of the Hamiltonian H_S , as described in the Appendix , and the Lindblad operators are given by [36]

A. Heat currents in a thermal transistor

$$\mathcal{L}_p[\rho] = \sum_{\omega} \gamma_p(\omega) \left[A_p(\omega) \rho A_p^\dagger(\omega) - \frac{1}{2} \{ \rho, A_p^\dagger(\omega) A_p(\omega) \} \right], \quad (5)$$

where $\gamma_p(\omega) = \mathcal{J}_p(\omega)[1 + n_p(\omega)]$ for $\omega > 0$ and $\gamma_p(\omega) = \mathcal{J}_p(|\omega|)n_p(|\omega|)$ for $\omega < 0$. The average number of excitations and the spectral density of the p -th reservoir are respectively $n_p(\omega) = [\exp\frac{\omega}{T_p} - 1]^{-1}$ and $\mathcal{J}_p(\omega)$. In all the numerical computations, we will choose Ohmic reservoirs characterized by a linear spectral density $\mathcal{J}_p(\omega) = \kappa_p \omega$ (at least in the range of working frequencies), using values of κ_p different for the three baths in order to suitably engineer the effect of the environments on the three qubits. It follows that $\gamma_p(0) = \lim_{\omega \rightarrow 0^+} \mathcal{J}_p(\omega)n_p(\omega) = \kappa_p T_p$. In the Appendix, a scheme of the transitions induced by the three thermal baths is also reported.

We remark that as we will consider a strong coupling between the three qubits (comparable or higher than the bare frequencies ω_p), we need the above microscopic approach to derive the Lindblad operators responsible of the non-unitary evolution of the density matrix, avoiding any extra simplification that can be somehow justified when the spin-spin interaction is much smaller than the bare frequencies of the qubits [36, 40]. In this limit, we cannot consider phenomenological master equations where the operators $A(\omega)$ are built starting from the eigenstates of the bare system Hamiltonian. For the z -axis Ising model, these coincide with the dressed eigenstates, while for the x -type this is not the case.

We also note that since H_{LS} commutes with H_S , it only leads to a renormalization of the unperturbed energy levels of H_S induced by the coupling with the reservoirs and that the steady state is independent on it.

The three temperatures of the environment will be in general chosen to be different, leading to out of thermal equilibrium steady states, which are not expected to be three-qubit thermal states. At the same time, we expect that each qubit will not thermalize (its own reduced state) to the temperature of its own reservoir because of the collective nature of the quantum dynamics.

III. QUANTUM THERMAL TRANSISTOR

The particular operating principle of an electronic transistor makes possible to regulate the currents at two of its terminals, that could take also very high values, regulating a much smaller current injected through a third terminal. This peculiarity made the transistor particularly suitable to build logic gates commonly used in nowadays electronic. We propose here a thermal analogue of this device able to amplify some of the heat currents circulating in a system as in Fig. 1. The control parameter that will play the role of the gate potential in an electronic transistor is the temperature T_M of the reservoir coupled to the *middle* qubit of frequency ω_M .

A straightforward way to take into account the heat flow in and out a quantum system [58], is to link the variation of its mean energy $\langle H_S \rangle$ to the sum of the heat currents J_p exchanged between the quantum system and each bath (no power comes from other external sources in our model):

$$\sum_p J_p = \frac{\partial \langle H_S \rangle}{\partial t}. \quad (6)$$

By substituting Eq. (4) in the previous expression, one can compute the current J_p that each thermostat exchanges with the system as

$$J_p = \text{Tr}(\mathcal{L}_p[\rho]H_S). \quad (7)$$

We note that at the steady state ρ_{ss} , it holds $\dot{\rho}_{ss} = 0$, so that the total energy is conserved in time. This implies that $\sum_p J_p = 0$. A minor remark concerns the fact that the Lamb shift term appearing in Eq. (4) does not contribute neither to the final expression of J_p neither to the steady state, so that the steady currents are independent on it. In the following, we always address steady configurations and we use J_p to indicate steady currents.

Following the geometry of the configuration of Fig. 1, we will refer to *left*, *middle* and *right* currents (J_L , J_M and J_R) to those exchanged, collectively, between the spin ring and, respectively, the left, the middle and the right thermostat. From now on, we assume that the hot reservoir, providing the energy to the system, is the left one, whereas the cold one, that adsorbs the heat flux, is the one placed to the right, and finally the bath in the middle acts as a control. Borrowing the familiar terminology of the bipolar transistor, the right qubit is playing the role of the emitter, while the left one of the collector and the middle one is indeed the analogue of the base.

The thermal transistor effect happens when a small change in the the control temperature T_M produce a significant variation of the two lateral currents in contrast with a tiny variation of J_M . To study the occurrence of this effect we define the differential thermal resistances

$$\chi_s = \left(\frac{\partial J_s}{\partial T_M} \right)_{T_s=\text{const}}^{-1}, \quad s = L, R, \quad (8)$$

and, as in the spirit of the electronic transistor [10], we introduce a dynamical amplification factor α_s , function of the control temperature T_M , defined as

$$\alpha_s = \frac{\partial J_s}{\partial J_M} = -\frac{\chi_s}{\chi_L + \chi_R}. \quad (9)$$

The adimensional parameters in Eq. (9) are the figures of merit used to have a quantitative benchmark of the presence of the thermal transistor effect and they satisfy the relation $\alpha_L + \alpha_R = -1$. In particular, for regions where $|\alpha_s| \gg 1$ one can infer that we are in presence of

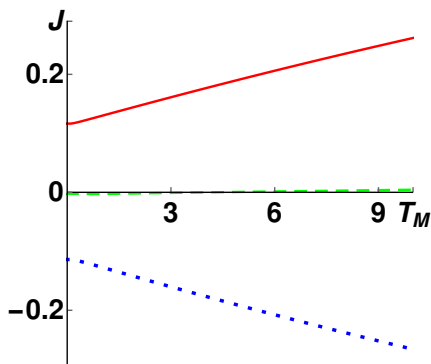


FIG. 2: (Color online) The three thermal currents defined in Eq. (7) (in units of $\kappa \Delta^2$) exchanged by the environments with the system as a function of the control parameter T_M (in units of Δ), when the system is described by an x -axis Ising model. The solid red line refers to J_L , the dashed green line to J_M and the blue dotted one to J_R . The parameters are $\omega_L = \Delta, \omega_M = 0.1 \Delta, \omega_R = 0.2 \Delta, \eta_{LM} = \eta_{MR} = \Delta, \eta_{LR} = 0, \kappa_L = \kappa_M = \kappa, \kappa_R = 100 \kappa, T_L = 10 \Delta$ and $T_R = 0.01 \Delta$. In the following figures, currents and temperatures are always meant, respectively, in units of $\kappa \Delta^2$ and Δ .

a strong amplification of the lateral currents in comparison to that controlled by the heat bath in central position. Therefore, it is evident that to amplify the thermal currents one of the two differential thermal resistances should be negative. We underline that this condition was already discussed in the context of non-linear lattices [16], three-terminal graphene devices [59] and band structured engineered silicene superlattices [60].

B. Thermal transistor in an x -axis Ising model

As said in Sec. II A the main case we want to discuss is when the three qubits are described by an x -axis Ising model. In particular, we choose open boundary condition, i.e. $\eta_{LR} = 0$.

In Fig. 2 we show the behavior of each current. In order to deal with adimensional quantities we plot the currents J_p in units of $\kappa \Delta^2$, where $\kappa = \kappa_L$ is the parameter characterizing the strength of the dissipation of the left qubit and $\Delta = \omega_L, \omega_L$ being assumed as the reference frequency. The currents are function of the temperature T_M , given in units of Δ . We observe that once expressed also κ_M and κ_R in units of κ , the steady state of Eq. (4) is invariant with respect to κ , while the currents are just proportional to it. Its value must just be small enough to guarantee the validity of the approximations used to derive the master equation of Eq. (4). In the following, all the values of temperatures are given in units of Δ , while for currents they are in units of $\kappa \Delta^2$. It is possible to appreciate in Fig. 2 how the thermal transistor effect manifests itself and how the amplification of J_L and J_R is continuously achieved.

We stress here the crucial role played by the non-

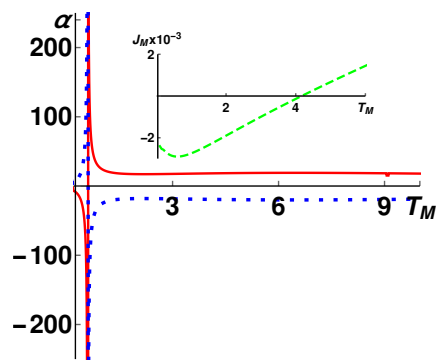


FIG. 3: (Color online) The amplification factors defined in Eq. (9) as a function of the control parameter T_M . The solid red line refers to α_L and the blue dotted one to α_R . In the inset, a zoom of J_M including its local minimum responsible of the divergence of the amplification factors. The parameters have the same values of Fig. 2.

equilibrium steady state. In fact, the presence of three environments at different temperatures plugged to distant sites of a magnetic system is the responsible of the three heat flows circulating into it. In particular, it is not surprising observing that even at $T_M = 0$ each of the currents has a non zero value.

In order to better describe the emergence of the thermal transistor effect, the amplification factors α_s are plotted in Fig. 3, where it is possible to see how the two lateral currents are amplified. Notably, around $T_M \simeq 0.600$, the amplification factor diverges, due to a local minimum of $J_M \simeq -2.90 \times 10^{-3}$. To this extent, we can circumscribe the best working region of this quantum thermal transistor to an interval of the control quantity centered around this value. However, a plateau is present where the amplification factors have values still significantly high. In particular, at $T_M \simeq 4.17$, where $J_M = 0$, $\alpha_L \simeq 18.3$. As a commentary, we notice that for this value of T_M , the reservoir M does not need to inject or absorb energy to maintain the system in the steady state, or in other words we can say that the central reservoir is in a situation of dynamical thermal equilibrium between the hot and the cold heat baths.

We also remark that it is easy to see that the right qubit is the one showing $\chi_R < 0$. We have thus shown how a purely quantum scenario can be used to implement a negative differential resistance device. Other choices of the values of the parameters entering either in H_S and in the dissipator of Eq. (4) give a behavior of the currents and of the amplifications analogous to the ones in Figs. 2 and 3. This has been observed in the case of asymmetric configurations.

C. Thermal transistor in a z -axis Ising model

In order to better assess the value of the model here proposed, we compare it with the model previously stud-

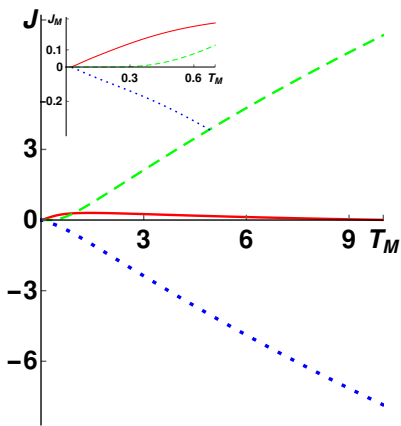


FIG. 4: (Color online) The three thermal currents defined in Eq. (7) exchanged by the environments with the system as a function of the control parameter T_M , when the system is described by a z -axis Ising model. The solid red line refers to J_L , the dashed green line to J_M and the blue dotted one to J_R . The parameters have the same values of Fig. 2. In the inset, a zoom including the working region of this setting.

ied in [43]. There, the thermal transistor effect had been observed in a range of temperatures much narrower than in our case. We put ourselves in the same zone of parameters identified in Fig. 2 and we look if it is possible to extend the working region to larger zones of temperatures as in the x -axis case.

In Fig. 4, we show that in the case of the z -axis Ising model the thermal transistor effect works only in a narrow interval of the control temperature, namely $T_M \in [0, 0.2]$. When moving to higher values of temperature, the effect completely vanishes, no matter how large the thermal gradient between the hot and cold heat baths is. In fact, in our analysis we have also increased the difference $T_R - T_L$ in comparison to what has been shown in [43] and observed that the current amplification is always achieved in the same narrow working region.

Recently, the appearance of current amplification has been discussed in a model based on a qubit-qutrit system. Also in this case, the thermal transistor works in a narrow interval of the control temperature in comparison to the x -type Ising model analyzed in Sec. III B, [44].

D. Local behavior

Here, we discuss the possibility to interpret the results of Fig. 2 on the basis of considerations involving only the local behavior of the qubits composing the spin ring. Firstly, we can have access to some local features introducing the reduced density matrix of any qubit, $\rho_p = \text{Tr}_{q,r \neq p}(\rho_{ss})$, where ρ_{ss} is the global steady state. We indicate with ρ_p^1 and ρ_p^0 , respectively, the populations of the excited and ground state of the p -th qubit. Each ρ_p is a mixed state in the local energy basis and such that we can define a local temperature for each qubit

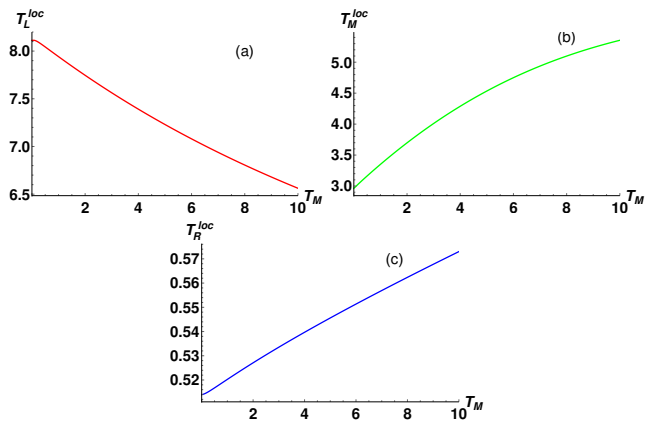


FIG. 5: (Color online) Local temperatures of the three qubits as defined in Eq. (10), as a function of the control parameter T_M . Plots (a), (b) and (c) refer, respectively, to the local temperature of the left, middle and right qubit. The parameters have the same values of Fig. 2.

($\rho_p^0 \geq \rho_p^1$), with respect to their free Hamiltonian, as:

$$T_p^{\text{loc}} = \frac{\omega_p}{\ln(\rho_p^0/\rho_p^1)}. \quad (10)$$

We plot in Fig. 5 the local temperatures of the qubits as a function of the control temperature T_M . It is clear that by increasing T_M , the temperature gradient between the L and M qubits decreases, in contrast to what happens between the pair of qubits M and R . In addition, the external qubits are never in thermal equilibrium with their respective environments, only the middle one reaches the equilibrium with the control thermostat M at $T_M \simeq 4.17$. For this value it holds $J_M = 0$ and $J_L = -J_R \simeq 0.179$. This means that all the heat injected by the hot reservoir into the system is transferred directly to the cold bath without any participation of the control bath.

Once analyzed the behavior of the local temperatures, we examine if we can qualitatively reproduce the behavior of the heat currents with the following local model. The three qubits are in contact with their local thermostats exactly as in our model, but the qubits do not interact between themselves. Instead, each qubit is also strongly coupled to another local thermal environment whose temperature is equal to (for any value of T_M) the temperature $T_p^{\text{loc}}(T_M)$ depicted in Fig. 5. The steady state of each qubit can be made close at will to the thermal state of temperature $T_p^{\text{loc}}(T_M)$ by suitably tuning the coupling between qubits and their own two local reservoirs. In this local model, the reduced state of each qubit is thus equal to the one obtained in our model, while the way each qubit dissipates is strongly different. In the local model the dissipation is governed by local Lindblad operators while in our model by collective ones, computed using the dressed states of H_S .

In Fig. 6 we compare the local currents with the exact ones of Fig. 2. We notice that in some cases, local currents well approximate the exact ones, like J_L , while in

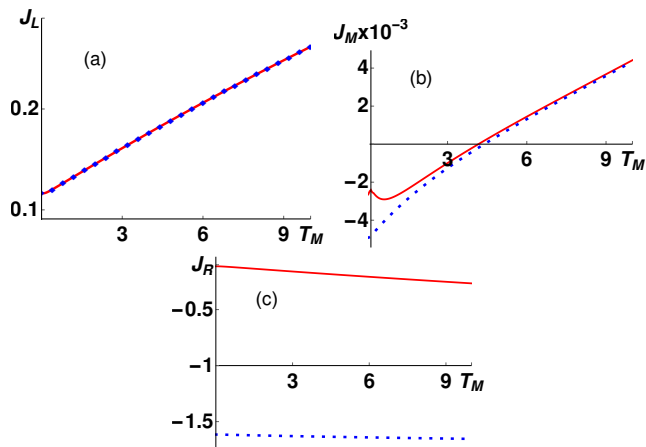


FIG. 6: (Color online) Comparison between the exact currents computed for the x -axis Ising model (red lines), the same ones of Fig. 2, and the currents obtained with the local model (dotted blue lines).

other they do not, like J_R . This is a clear indication of the relevant role played by the collective behavior of the spin ring when it exchanges heat with the local thermostats. The local temperatures induced by the collective dynamics are thus, in general, not enough by themselves to catch all the physics of this collective exchange and of the occurrence of the thermal transistor effect. In particular, we stress the absence of a local minimum for J_M , around which we observed the best performance of the device.

IV. ROBUSTNESS AGAINST PERTURBATIONS

The results reported in the previous sections show how to build a quantum thermal transistor operating on a wide range of temperatures and starting from a microscopic derivation, with a potential implementation over some feasible physical settings. However, in any real physical implementation of an Ising Hamiltonian, spurious and undesired couplings pointing along different directions of the desired axis for the interaction could occur. This could entail a loss of the thermal transistor effect. Obviously, in any controlled setup, those interactions can be considered as small fluctuations and treated by means of perturbative corrections to the system Hamiltonian H_S . Nevertheless, in order to pursue our microscopical description of the effect and be precise, we use the full model for the three qubits as in Eq. (2), introducing time by time more complex interactions and studying to which extent they alter the amplification performances.

In order to substantiate the process illustrated so far, we consider a physical implementation where the real axis of the interaction term of the model can differ from the expected one (indicated with k in the following) [49], and we compute the amplification factors, $\alpha_s(\lambda^i, \lambda^j)$, that are

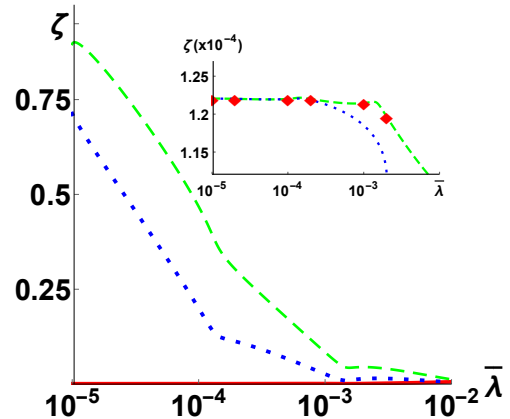


FIG. 7: (Color online) The ratio ζ defined in Eq. (12) for the x -type Ising model, as a function of the mean value of the spurious couplings $\bar{\lambda}^{i,j}$. The dashed green line refers to ζ^z , the blue dotted one to ζ^y and the red solid line takes into account perturbations with both λ^y and $\lambda^z \neq 0$ but with the same mean value, namely $\zeta^{y,z}$. In the inset, the ratio ζ for the z -type Ising model. Here, the dashed green line refers to ζ^x , coinciding with ζ^y (red diamonds). The blue dotted one refers to $\zeta^{x,y}$ and is obtained imposing λ^y and $\lambda^z \neq 0$ with the same mean value. The parameters of the unperturbed configuration are the same as in Fig. 2.

now functions of the couplings, λ^i and λ^j , along the other two possible polarization directions i and j , and they may assume a different value from the unperturbed one. Only the coupling between the qubits L and M and between the qubits R and M are perturbed, while the coupling between the qubits L and R is maintained equal to zero as before.

To obtain a statistical detailed analysis we assume that the values of the perturbations are normally distributed and we evaluate the averaged amplification factors

$$\bar{\alpha}_s^{i,j} = \int d\lambda^i d\lambda^j \alpha_s(\lambda^i, \lambda^j) \mathcal{N}(\bar{\lambda}^{i,j}, \Sigma^{i,j}), \quad (11)$$

where $s = L, R$, and $\mathcal{N}(\bar{\lambda}^{i,j}, \Sigma^{i,j})$ is the bivariate Gaussian distribution of the perturbations. It is centered around their mean values $\bar{\lambda}^{i,j} = (\bar{\lambda}^i, \bar{\lambda}^j)$, with covariance matrix given by $\Sigma^{i,j} = \text{diag}(\Sigma^i, \Sigma^j)$. In particular, we choose that the spurious interactions can deviate of around 10% from their mean value, i.e. $\Sigma^i = 0.1\bar{\lambda}^i$.

As a tool to investigate the effect of small perturbations, we define the ratio

$$\zeta^{i,j} = \frac{\bar{\alpha}_L^{i,j}}{\alpha_L^{\text{unp}}}, \quad (12)$$

where α_L^{unp} represents the value of the left amplification factor obtained in the absence of perturbation. If only one additional coupling of the type $\sigma_p^i \sigma_q^i$ perturbs the main interaction term $\sigma_p^k \sigma_q^k$, the above ratio is indicated

with ζ^i . For the sake of clarity, we point out that another quantity analogue to $\zeta^{i,j}$ can be in principle defined using the amplification factor of the right current α_R . Nevertheless, its value depends on α_L in a simple way, such that for any T_M this choice would lead to analogues dampings of $\zeta^{i,j}$ as function of the strength of the perturbation, $\bar{\lambda}^{i,j}$.

In Fig. 7 we show the quantity ζ as a function of the average strength of 3 types of typical perturbations that can occur in both settings discussed in Section III. Since α_L^{unp} can diverge for a certain value of the control temperature T_M , we fix it equal to $T_M = 0.650$, close enough the one where the divergence appears in order to have $\alpha_L^{\text{unp}} \gg 1$ but where it is still finite, being $\alpha_L^{\text{unp}} \simeq 1.42 \times 10^3$. We stress here that the value of T_M in the presence of perturbations is kept the same of the unperturbed case. The quantity ζ is close to unity when the system still operates as a quantum transistor close to its unperturbed value α_L^{unp} but it vanishes as soon as the perpendicular couplings become more intense.

As it is apparent from the plot, the x -axis and z -axis Ising models show a completely opposite behavior in the presence of perturbations. Indeed, despite the fact that both the models have been perturbed around a quite optimal configuration, the x -axis model still shows the thermal transistor effect for extra couplings small enough. In contrast, the possibility to achieve a current amplification with the z -axis Ising model is completely lost in the presence of infinitesimal couplings among the spin in any direction perpendicular to the wanted interaction axis. Our numerical evidences only allow us to see that ζ is extremely low for values of the extra couplings larger than ten millionths of the one along the z -axis, but we cannot surmise how the unperturbed value is restored for smaller values of the spurious coupling $\bar{\lambda}^{i,j}$.

We also provide a qualitative mathematical explanation of this phenomenon which resides on the structure of the couplings between the qubits. In fact, as pointed out when discussing the two possible configurations, a coupling commuting with the bare Hamiltonian affects only the eigenfrequencies of the systems and it leaves unchanged the eigenstates entering in the definition of the operators $A(\omega)$, that are essential to derive the dissipative dynamics of Eq. (4). Adding a perpendicular coupling, not commuting with the bare part of H_S completely alters their structure and it imposes to consider the dressed-state basis to write the $A(\omega)$, that typically differs from the bare-state basis one.

V. CONCLUSIONS

In this paper, we have addressed the design and the possible physical implementation of a quantum thermal transistor. This novel device acts on thermal currents as a bipolar electronic transistor does with electric currents, providing an amplification of the collector's and emitter's currents by a proper tuning of the gate potential,

while the corresponding gate current is order of magnitude lower than the other two and practically constant.

Our model proposes a system of three qubits strongly interacting among them and each of them in contact with a different thermal reservoir. This setting imposes non-equilibrium dissipative dynamics that entail the presence of non-vanishing steady state currents flowing into the system via bath induced transitions. We have focused our attentions on a particular system that can lead to a feasible realization on several experimental platforms, such as molecular nanomagnets and few-body spin chains, and we have referred to this model as the spin-ring model.

In particular, we have devoted our efforts to describe how a quantum thermal transistor works in a scenario where a more complex spin-spin coupling is present, in comparison to a previous model recently presented in [43]. Throughout the paper, we have referred to these two models as the x -type Ising model and the z -type Ising model. The former is characterized by an interaction Hamiltonian not commuting with the bare one, or in other words the magnetic field acting on the three spins is perpendicular to the direction along which the spins interact; the latter, instead, is a model where magnetic fields and interaction are longitudinal, so that the two contributions of the system Hamiltonian commute.

Choosing as control parameter the temperature of the heat bath directly coupled to the middle qubit, we have shown that the x -type spin ring operates as a thermal transistor over a wider range of temperatures in comparison to the z -type one. The significant amplification of the lateral currents has been justified in the context of devices characterized by negative differential thermal resistance [16, 59, 60] and by means of the collective dynamics. In fact, considering a naive local model for the system, that partially takes into account collective phenomena, cannot explain the whole behavior exhibited by our model. Finally, we have discussed the robustness of both the possible implementations against spurious and uncontrollable couplings stemming from the magnetic interaction between the different pairs of the effective spins of the magnetic ring. The results of exact numerical computations suggest that, for reasonably small perturbations, the x -type molecule can be steered acting on the control temperature to behave still as a thermal transistor around its unperturbed configuration. In contrast, our computations show that the z -type molecule is really fragile in presence of those kinds of perturbations.

As final remarks, we would like to point out that even if we have performed a microscopic derivation of master equation describing the dynamics of the system, overriding any phenomenological simplification, a deeper comprehension of the very quantum effects conducting to such current amplification is still lacking. It could be matter of future investigation the role of system criticality and of the dissipation mechanism and how they contribute and compete in order to state a general scheme to build a quantum thermal transistor.

Acknowledgments

A.M. acknowledges the ‘‘R egion Bourgogne-Franche-Comt e’’ for financial support throughout the mobility grant N. 2017Y-06400. B.B. acknowledges the support by the French ‘‘Investissements d’Avenir’’ program, project ISITE-BFC (contract ANR-15-IDEX-03). A.M. thanks Heinz-Peter Breuer for useful comments and Elena Servida for discussions about semiconductor electronics. B.B. thanks Benedetto Militello and David Vienneot for helpful comments.

Appendix: Spectrum of the system Hamiltonian in the x -type Ising model.

In this appendix we give a sketch of the diagonalization of the system Hamiltonian introduced in Eq. (2) and used to obtain the thermal transistor effect discussed throughout the paper. In particular, we focus on the case of the x -type Ising model with the left and right qubits not interacting, i.e. $\eta_{LR} = 0$. The matrix of a system composed by three qubits with different splitting in a magnetic field with a transverse Ising interaction reads:

$$\frac{1}{2} \begin{pmatrix} \Omega_{LM} + \omega_R & 0 & 0 & \Lambda_{MR}^x & 0 & 0 & \Lambda_{LM}^x & 0 \\ 0 & \Omega_{LM} - \omega_R & \Lambda_{MR}^x & 0 & 0 & 0 & 0 & \Lambda_{LM}^x \\ 0 & \Lambda_{MR}^x & \Omega_{LR} - \omega_M & 0 & \Lambda_{LM}^x & 0 & 0 & 0 \\ \Lambda_{MR}^x & 0 & 0 & \omega_L - \Omega_{MR} & 0 & \Lambda_{LM}^x & 0 & 0 \\ 0 & 0 & \Lambda_{LM}^x & 0 & -\omega_L + \Omega_{MR} & 0 & 0 & \Lambda_{MR}^x \\ 0 & 0 & 0 & \Lambda_{LM}^x & 0 & \omega_M - \Omega_{LR} & \Lambda_{MR}^x & 0 \\ \Lambda_{LM}^x & 0 & 0 & 0 & 0 & \Lambda_{MR}^x & -\Omega_{LM} + \omega_R & 0 \\ 0 & \Lambda_{LM}^x & 0 & 0 & \Lambda_{MR}^x & 0 & 0 & -\Omega_{LM} - \omega_R \end{pmatrix}, \quad (\text{A.1})$$

where we have assumed $\eta_{qp} = \eta_{pq}$ and for shorthand we have introduced $\Omega_{pq} = \omega_p + \omega_q$ and $\Lambda_{pq}^x = \eta_{pq}\lambda^x$ with $p, q = L, M, R$.

The secular equation of Eq. (A.1) can be reduced to a quartic equation, leading to four pairs of energy eigenvalues equal in modulus. We can, therefore, decompose H_S in the base where it is diagonal, $H_s = \sum_{i=1}^8 \epsilon_i |\epsilon_i\rangle\langle\epsilon_i|$, where we have ordered the energy eigenvalues using the following notation $\epsilon_8 \leq \epsilon_7 \leq \dots \leq \epsilon_1$ and $\epsilon_{9-i} = -\epsilon_i, \forall i$.

Introducing the computational basis, defined as the tensor product $|l_L l_M l_R\rangle$, of all the dispositions of the eigenvectors of the three σ_p^z , i.e. $\sigma_p^z |l_p\rangle = (-1)^{(l_p+1)} |l_p\rangle$, with $l_p = 0, 1$ and $p = L, M, R$, the eigenvectors of H_S , found for the main case discussed in the paper (Sec. III B), are:

$$\begin{aligned} |\epsilon_1\rangle &= -a_1|111\rangle - a_2|100\rangle - a_3|010\rangle - a_4|001\rangle \\ |\epsilon_8\rangle &= +a_1|000\rangle - a_2|011\rangle + a_3|101\rangle - a_4|110\rangle \\ |\epsilon_2\rangle &= +b_1|000\rangle + b_2|011\rangle + b_3|101\rangle + b_4|110\rangle \\ |\epsilon_7\rangle &= +b_1|111\rangle - b_2|100\rangle + b_3|010\rangle - b_4|001\rangle \\ |\epsilon_3\rangle &= +c_1|000\rangle - c_2|011\rangle - c_3|101\rangle + c_4|110\rangle \\ |\epsilon_6\rangle &= -c_1|111\rangle - c_2|100\rangle + c_3|010\rangle + c_4|001\rangle \\ |\epsilon_4\rangle &= +d_1|111\rangle - d_2|100\rangle - d_3|010\rangle + d_4|001\rangle \\ |\epsilon_5\rangle &= -d_1|000\rangle - d_2|011\rangle + d_3|101\rangle + d_4|110\rangle \end{aligned}, \quad (\text{A.2})$$

where the 16 real coefficients a_i, b_i, c_i, d_i with $i = 1, 2, 3, 4$ in the above expressions are functions of the parameters entering in the Hamiltonian. In all the numerical trials, we have found the same above structure for the eigenvectors, all the coefficients being real.

It is worth noting that the above states have well-

defined parity and that the states with opposite energy have different parity. In fact, it is easy to check it by measuring the parity operator $P = \sigma_L^z \otimes \sigma_M^z \otimes \sigma_R^z$ on any term appearing in $|\epsilon_i\rangle$.

Finally, we report in Table I the transitions mediated by any thermal reservoir. It is worth noting that we write here only the transitions that can be interpreted as the emission of a photon in the usual context of quantum optics, since they involve states with a positive energy difference between the initial and the final value.

TABLE I: The possible transitions of positive frequency mediated by any of the three thermal baths by means of the interaction operator σ_p^x for the case of Sec. III B. The first column gives the initial states, starting from the one with highest energy, whilst the other columns specify the qubit operator coupled to the corresponding thermal reservoir as prescribed by Eq. (3), and the final states connected to the initial ones.

	σ_L^x	σ_M^x	σ_R^x
$ \epsilon_1\rangle$	$ \epsilon_2\rangle, \epsilon_3\rangle, \epsilon_5\rangle$	$ \epsilon_2\rangle, \epsilon_3\rangle, \epsilon_5\rangle, \epsilon_8\rangle$	$ \epsilon_2\rangle, \epsilon_3\rangle, \epsilon_5\rangle$
$ \epsilon_2\rangle$	$ \epsilon_4\rangle, \epsilon_6\rangle$	$ \epsilon_4\rangle, \epsilon_6\rangle, \epsilon_7\rangle$	$ \epsilon_4\rangle, \epsilon_6\rangle$
$ \epsilon_3\rangle$	$ \epsilon_4\rangle, \epsilon_7\rangle$	$ \epsilon_4\rangle, \epsilon_6\rangle, \epsilon_7\rangle$	$ \epsilon_4\rangle, \epsilon_7\rangle$
$ \epsilon_4\rangle$	$ \epsilon_8\rangle$	$ \epsilon_5\rangle, \epsilon_8\rangle$	$ \epsilon_8\rangle$
$ \epsilon_5\rangle$	$ \epsilon_6\rangle, \epsilon_7\rangle$	$ \epsilon_6\rangle, \epsilon_7\rangle$	$ \epsilon_6\rangle, \epsilon_7\rangle$
$ \epsilon_6\rangle$	$ \epsilon_8\rangle$	$ \epsilon_8\rangle$	$ \epsilon_8\rangle$
$ \epsilon_7\rangle$	$ \epsilon_8\rangle$	$ \epsilon_8\rangle$	$ \epsilon_8\rangle$

-
- [1] S. Carnot, *Reflexions sur la Puissance Motrice du Feu*, (Bachelier Libraire, Paris, 1824).
- [2] G. Gemma, M. Michel, and G. Mahler, *Quantum Thermodynamics* (Springer, Heidelberg, 2004).
- [3] H. T. Quan, Yu-xi Liu, C. P. Sun, and F. Nori, Phys. Rev. E **76**, 031105 (2007).
- [4] R. Uzdin, A. Levy, and R. Kosloff, Phys. Rev. X **5**, 031044 (2015).
- [5] J. Roßnagel, S. T. Dawkins, K. N. Tolazzi, O. Abah, E. Lutz, F. Schmidt-Kaler, and K. Singer, Science **352**, 325 (2016).
- [6] B. Bellomo and M. Antezza, Phys. Rev. A **91**, 042124 (2015).
- [7] B. Leggio, B. Bellomo, and M. Antezza, Phys. Rev. A **91**, 012117 (2015).
- [8] M. Campisi, J. Pekola, and R. Fazio, New J. Phys. **17**, 035012 (2015).
- [9] R. Alicki and D. Gelbwaser-Klimovsky, New J. Phys. **17**, 115012 (2015).
- [10] J. Bardeen, and W. H. Brattain, Phys. Rev. **74**, 230 (1948).
- [11] J. Millman, *Microelectronics* (McGraw-Hill, New York, 1983).
- [12] M. Michel, G. Mahler, and J. Gemmer, Phys. Rev. Lett. **95**, 180602 (2005).
- [13] D. Manzano, M. Tiersch, A. Asadian, and H. J. Briegel, Phys. Rev. E **86**, 061118 (2012).
- [14] M. Terraneo, M. Peyrard, and G. Casati Phys. Rev. Lett. **88**, 094302 (2002).
- [15] B. Li, L. Wang, and G. Casati, Phys. Rev. Lett. **93**, 184301 (2004).
- [16] B. Li, L. Wang, and G. Casati, Appl. Phys. Lett. **88**, 143501 (2006).
- [17] P. Ben-Abdallah and S.-A. Biehs Phys. Rev. Lett. **112**, 044301 (2014).
- [18] K. Joulain, Y. Ezzahri, J. Drevillon, and P. Ben-Abdallah, Appl. Phys. Lett. **106**, 133505 (2015).
- [19] L. Wang and B. Li, Phys. Rev. Lett. **99**, 177208 (2007).
- [20] N. Li, J. Ren, L. Wang G. Zhang, P. Hänggi, and B. Li, Rev. Mod. Phys. **84**, 1045 (2012).
- [21] C. W. Chang, D. Okawa, A. Majumdar, and A. Zettl, Science **314**, 1121 (2006).
- [22] W. Kobayashi, Y. Teraoka, and I. Terasaki, Appl. Phys. Lett. **95**, 171905 (2009).
- [23] R. Scheibner, M. Knig, D. Reuter, A. D. Wieck, C. Gould, H. Buhmann, and L. W. Molenkamp, New J. Phys. **10**, 083016 (2008).
- [24] S. Borlenghi, S. Lepri, L. Bergqvist, and A. Delin, Phys. Rev. B **89**, 054428 (2014).
- [25] P. J. van Zwol, K. Joulain, P. Ben-Abdallah, and J. Chevrier, Phys. Rev. B **84**, 161413(R) (2011).
- [26] P. J. van Zwol, L. Ranno, and J. Chevrier, Phys. Rev. Lett. **108**, 234301 (2012).
- [27] E. Nefzaoui, K. Joulain, J. Drevillon, and Y. Ezzahri, Appl. Phys. Lett. **104**, 103905 (2014).
- [28] J. Ordonez-Miranda, K. Joulain, D. De Sousa Meneses, Y. Ezzahri, and J. Drevillon, J. Appl. Phys. **122**, 093105 (2017).
- [29] R. Hanson and D. D. Awschalom, Nature (London) **453**, 1043 (2008).
- [30] Z. Yu and S. Fan, Nat. Photonics **3**, 91 (2009).
- [31] E. Mascarenhas, D. Gerace, D. Valente, S. Montangero, A. Auffèves, and M. F. Santos, Eur. Phys. Lett. **106**, 54003 (2014).
- [32] E. Mascarenhas, M. F. Santos, A. Auffèves, and D. Gerace Phys. Rev. A **93**, 043821 (2016).
- [33] J. Hwang, M. Pototschnig, R. Lettow, G. Zumofen, A. Renn, S. Gtzinger, and V. Sandoghdar, Nature (London) **460**, 76 (2009).
- [34] O. V. Astafiev, A. A. Abdumalikov, Jr., A. M. Zagoskin, Yu. A. Pashkin, Y. Nakamura, and J. S. Tsai, Phys. Rev. Lett. **104**, 183603 (2010).
- [35] J.-H. Jiang, M. Kulkarni, D. Segal, and Y. Imry, Phys. Rev. B **92**, 045309 (2015).
- [36] H.-P. Breuer and F. Petruccione, *The Theory of Open Quantum Systems* (Oxford University Press, Oxford, 2002).
- [37] G. Schaller, *Open Quantum Systems Far from Equilibrium* (Springer, Heidelberg, 2014).
- [38] N. Linden, S. Popescu, and P. Skrzypczyk, Phys. Rev. Lett. **105**, 130401 (2010).
- [39] Z.-X. Man, and Y.-J. Xia, Phys. Rev. E **96** 012122 (2017).
- [40] T. Werlang, M. A. Marchiori, M. F. Cornelio, and D. Valente, Phys. Rev. E **89**, 062109 (2014).
- [41] T. Chen and X.-B. Wang, Physica E (Amsterdam) **72**, 58 (2015).
- [42] J. Ordonez-Miranda, Y. Ezzahri, and K. Joulain, Phys. Rev. E **95**, 022128 (2017).
- [43] K. Joulain, J. Drevillon, Y. Ezzahri, and J. Ordonez-Miranda, Phys. Rev. Lett. **116**, 200601 (2016).
- [44] B.-Q. Guo, T. Liu, and C.-S. Yu, Phys. Rev. E **98**, 022118 (2018).
- [45] J. Bartolomè, F. Luis, and J. F. Fernández, editors, *Molecular Magnets: Physics and Applications, NanoScience and Technology* (Springer, 2014).
- [46] L. Amico, R. Fazio, A. Osterloh, and V. Vedral, Rev. Mod. Phys. **80**, 517 (2008).
- [47] A. A. Khajetoorians, J. Wiebe, B. Chilian, S. Lounis, S. Blügel, and R. Wiesendanger, Nat. Phys. **8**, 497 (2012).
- [48] R. Toskovic, R. van den Berg, A. Spinelli, I. S. Eliens, B. van den Toorn, B. Bryant, J.-S. Caux and, A. F. Otte, Nat. Phys. **12**, 656 (2016).
- [49] D. Bitko, T. F. Rosenbaum, and G. Aeppli, Phys. Rev. Lett. **77**, 940 (1996).
- [50] N. Roch, S. Florens, V. Bouchiat, W. Wernsdorfer, and F. Balestro, Nature **453**, 633 (2008).
- [51] R. Coldea, D. A. Tennant, E. M. Wheeler, E. Wawrzynska, D. Prabhakaran, M. Telling, K. Habicht, P. Smeibidl, and K. Kiefer, Science **327**, 177 (2010).
- [52] F. Troiani and P. Zanardi, Phys. Rev. B **88**, 094413 (2013).
- [53] G. Salvatori, A. Mandarino, and M. G. A. Paris, Phys. Rev. A **90**, 022111 (2014).
- [54] M. D. Jenkins, Y. Duan, B. Diosdado, J. J. García-Ripoll, A. Gaita-Ariño, C. Giménez-Saiz, P. J. Alonso, E. Coronado, and F. Luis, Phys. Rev. B **95**, 064423 (2017).
- [55] I. Dzyaloshinsky, J. Phys. Chem. Solids **4**, 241 (1958).
- [56] T. Moriya, Phys. Rev. **120**, 91 (1960).
- [57] K.-Y. Choi, Y.H. Matsuda, H. Nojiri, U. Kortz, F. Husain, A.C. Stowe, C. Ramsey, and N.S. Dalal, Phys. Rev. Lett. **96**, 107202 (2006).
- [58] R. Kosloff, Entropy **15**, 2100 (2013).

- [59] Y. Wu, D. B. Farmer, W. Zhu, S.-J. Han, C. D. Dimitrakopoulos, A. A. Bol, P. Avouris, and Y.-M. Lin, *ACS Nano* **6**, 2610 (2012).
- [60] C.-H. Chen, W.-W. Li, Y.-M. Chang, C.-Y. Lin, S.-H. Yang, Y. Xu, and Y.-F. Lin, *Phys. Rev. Appl.* **10**, 044047 (2018).